HHS Public Access

Author manuscript

J Clin Ultrasound. Author manuscript; available in PMC 2020 October 23.

Published in final edited form as:

J Clin Ultrasound. 2016 May ; 44(4): 221–230. doi:10.1002/jcu.22333.

Predictors of Incipient Dysfunction of All Cardiac Chambers After Treatment of Metastatic Renal Cell Carcinoma by Tyrosine Kinase Inhibitors

Sherif Moustafa, MBBCh[1], **Thai H. Ho, MD, PhD**[2], **Parth Shah, BSc**[1], **Katie Murphy, MD**[1], **Bhargava K. Nelluri, MD**[1], **Howard Lee, MD, PhD**[1], **Susan Wilansky, MD**[1], **Farouk Mookadam, MD**[1]

[1]Division of Cardiovascular Diseases, Department of Medicine, Mayo Clinic, Arizona, AZ

[2]Division of Hematology/Oncology, Department of Medicine, Mayo Clinic, Arizona, AZ

Abstract

Purpose.—We aimed to explore the hypothesis that early subclinical cardiac chamber dysfunction secondary to tyrosine kinase inhibitors (TKIs) in patients with metastatic renal cell carcinoma could be signaled by abnormal cardiac mechanics demonstrated by velocity vector imaging.

Methods.—Echocardiographic images were acquired from the apical views in 23 metastatic renal cell carcinoma patients. All patients had baseline and at least a 3-month follow-up echocardiogram after receiving TKI therapy. Subendocardial borders of all the cardiac chambers were traced to obtain volumetric and deformation indices.

Results.—Mean age was 67 ± 9 years with 92% men. The right ventricle peak systolic global longitudinal strain (GLε) and strain rate were significantly lower after TKIs (−23.49 ± 5.1 versus −19.81 ± 5.5, $p = 0.002$ and −1.52 ± 0.52 versus −1.24 ± 0.35 $p = 0.02$, respectively). LV GLε was not statistically different. Volumetric and deformation indices showed a minimal decrease of the right atrium reservoir and conduit functions, and no significant changes of left atrial function.

Conclusions.—The right heart exhibited greater strain changes than the left heart after TKI treatment. The implications of these findings and their potential significance warrant further work.

Keywords

tyrosine kinase inhibitors; renal cell carcinoma; velocity vector imaging; cardiac chambers; function; echocardiography

INTRODUCTION

Renal cell carcinoma (RCC) is the most common malignant kidney neoplasm. It has a proclivity for metastasis with approximately 30% of patients already with metastases at the time of first presentation.[1,2] In the setting of metastatic disease, contemporary treatments of

Correspondence to: S. Moustafa.

metastatic RCC (mRCC) include inhibitors of vascular endothelial growth factor receptor (VEGFR) and of mammalian target of rapamycin.[1,2] Targeted therapies, mainly tyrosine kinase inhibitors (TKIs), have had a significant impact on the treatment of mRCC. TKIs improved quality of life with reduced adverse effects compared with conventional chemotherapy.[3–5]

Protein kinases contain a conserved ATP binding pocket, which is a key region targeted by inhibitors. The mechanism of TKIs includes inhibition of growth factor receptors such as VEGFR, platelet-derived growth factor receptor, stem cell factor KIT receptor, and other signaling pathways. This leads to significant deceleration of tumor cell proliferation and angiogenesis.[4–6] However, the conservation of the ATP binding pocket may lead to "off-target" effects on unintended kinases, and TKIs have several side effects including gastrointestinal upset, hypothyroidism, bone marrow toxicity, hand-foot syndrome, and stomatitis. Furthermore, cardiotoxicity such as hypertension, congestive heart failure (CHF), drop of left ventricular ejection fraction (LVEF) by 10%, myocardial ischemia, and arterial thromboembolic events has been reported. In meta-analyses of randomized control trials, the incidence of fatal adverse events and CHF related to VEGFR TKIs were 1.5% and 2.4%, respectively. However, the exact risk of cardiac events and the potential for recovery are still unknown.[2–9]

Velocity vector imaging (VVI) is a relatively novel tool that can assess myocardial mechanics using a sophisticated technique that involves endocardial border tracking achieved with Fourier techniques. It permits a multidirectional exploration of myocardial motion in an angle-independent manner. This validated technique is promising for evaluating cardiac chamber global and regional function because it is relatively load-independent.[10–15] We aimed to explore the hypothesis that early subclinical cardiac chamber dysfunction, secondary to TKIs in patients with mRCC, could be signaled by abnormal mechanics assessed by VVI.

MATERIALS AND METHODS

Study Population

Between January 2012 and December 2014, 56 consecutive patients with mRCC were retrospectively screened. Patients with mRCC referred for echocardiograms were included. Inclusion criteria were as follows: (1) mRCC treated with TKIs; (2) baseline (pre-TKI treatment) transthoracic echocardiogram (TTE); (3) at least 3 months post-TKI commencement TTE; (4) age ≥18 years. Patients who received a regimen other than TKIs (N =14) or with uninterpretable echographic images were excluded (N = 19). The study complied with the Declaration of Helsinki and was approved by the Institutional Review Board.

Conventional Echocardiography

All patients underwent comprehensive two-dimensional Doppler and tissue Doppler imaging echocardiography. The images were acquired from the standard views for calculation of dimensions, volumes, and mass. Complete visualization of all cardiac chambers, including

both atria, was ensured. All measurements were achieved according to the American Society of Echocardiography guidelines.[16–18]

Velocity Vector Imaging

Two-dimensional echocardiography gray-scale images were stored as DICOM (Digital Imaging and Communications in Medicine) format and analyzed using a VVI tracking system (Syngo US Workstation; Siemens Medical Solutions, Inc., Malvern, PA). For VVI analysis, the three apical views were used for the left ventricle (LV) and the apical four-chamber view was used for the right ventricle (RV). Both RV/LV subendocardial borders were traced and tracked by the software along the borders in order to achieve average global systolic longitudinal strain (GLε) and strain rate (SR). Manual adjustments of the tracking points were attained as appropriate. Inadequately tracked segments were excluded (Figure 1).[11,13,15,19]

Right and left atrial (RA and LA) subendocardial borders were outlined and tracked by the software in the apical four-chamber view. Manual adjustments of the tracking points were accomplished as appropriate. ε and SR values were obtained through the cardiac cycle (Figure 2).[10,13,14,19]

Computer-generated LA/RA volume curves were produced by continuous tracing of the atrial endocardium. Subsequently, atrial ejection fraction (EF) and the ensuing volume indices were calculated: maximum atrial volume (AVmax), minimal atrial volume (AVmin), and the atrial volume before the atrial contraction (AVpre-a) (Figure 2).

Furthermore, dynamic atrial function indices were calculated from the measured volumes[10,19–26]:

1. Atrial reservoir function:

Filling volume = (AVmax – AVmin).

Expansion index = ([AVmax – AVmin]/ AVmin)×100.

Diastolic emptying index = ([AVmax – AVmin]/AVmax)×100.

2. Atrial conduit function:

Passive emptying percent of total emptying = ([AVmax – AVpre–a]/[AVmax – AVmin]) ×100.

Passive emptying index = ([AVmax – AVpre–a]/AVmax)×100.

3. Atrial booster pump function:

Active emptying percent of total emptying = ([AVpre–a – AVmin]/[AVmax – AVmin])×100.

Active emptying index = ([AVpre–a –AVmin]/AVpre–a)×100.

ε and SR curves were employed for analysis. Peak positive ε (ε_{Pos}), peak negative ε (ε_{Neg}), peak early negative SR ($SR_{EarlyNeg}$), peak late negative SR ($SR_{LateNeg}$), and peak positive SR (SR_{Pos}) values were calculated. Consequently, ε_{Neg} (matching the atrial booster pump function) and ε_{Pos} (matching the conduit function) were computed. The SR values ($SR_{LateNeg}$, SR_{Pos}, and $SR_{EarlyNeg}$), representing atrial contraction, beginning of ventricular systole, and beginning of ventricular diastole, were gauged (Figure 2).[10,19–26]

Statistical Analysis

Data are presented as mean ± SD. Student's *t* test was used to compare different variables. Pearson correlation analysis was performed to test the correlations between the variables. *p* value < 0.05 was considered statistically significant. After a delay of 8 weeks from the initial appraisal, intra- and interobserver variability was evaluated by submitting arbitrary selected images for analysis and measurement by another observer blinded to the earlier results. Ten individuals were randomly selected for this analysis. Variability was calculated as the absolute alteration among the corresponding repetitive measurements as a percent of their mean.

RESULTS

Patient Characteristics

Baseline characteristics of the patients are summarized in Table 1. The study enrolled 23 subjects with a mean age of 67 ± 9 years (range 46–85 years). Four patients had a history of transient ischemic attacks and two had prior percutaneous coronary intervention, but no myocardial infarction. The incidence of pre-existing hypertension was high (43%). No patients had a history of CHF.

The TKI pazopanib (800 mg orally once daily) was the agent most frequently used, followed by sunitinib (50 mg orally for 4 weeks, then stopped for 2 weeks), and axitinib (5 mg orally twice daily) (Table 1). Three patients were switched from axitinib to pazopanib due to intolerance (n = 1) and/or lack of adequate response (n = 2).

Clinical Cardiotoxicity

Four patients (18%) developed new onset hypertension and two (9%) had worsening of pre-existing hypertension while on therapy. All were receiving either pazopanib (n = 4) or sunitinib (n = 2). Sixty-seven percent of the hypertensive patients required therapy with at least a single antihypertensive agent, and 33% of patients needed two or more agents (Table 1). No patients developed new onset CHF.

No significant differences were noted in regards to biomarkers post-TKIs (i.e., serum levels of brain natriuretic peptide and troponins; data not shown).

Conventional Indices of Cardiac Function

The median interval between baseline echocardiography and follow-up was 169 days.

There was no significant decrease in mean LVEF, RV fractional area change (FAC) %, and tricuspid annular plane systolic excursion (TAPSE) with TKI therapy. Global S′ wave of the mitral valve was significantly lower in the post-TKIs than in the pre-TKIs group. Differences in the remaining systolic and diastolic function variables between groups were not statistically significant (Table 2).

LV/RV Global Longitudinal Deformation Indices

LV peak systolic GLε and SR did not statistically change. However, RV peak systolic GLε was significantly lower post-TKIs ($p = 0.002$).[27] RV peak systolic SR was significantly lower as well ($p = 0.02$) (Table 3). No significant correlations were noted between LV/RV global longitudinal deformation indices and variables of LV/RV systolic and diastolic functions (data not shown).

Dynamic Global Atrial Function Applying Volumetric Indices

VVI data for global atrial function are summarized in Table 4. LA volumes and EF did not change significantly with TKIs. Dynamic global function indices revealed that atrial filling during ventricular systole (reservoir function), passive LV filling in early diastole (conduit function), and atrial contraction (booster pump function) were similar pre- and post-TKI therapy.

RA volumes and EF did not change significantly with TKIs. Nonetheless, dynamic global function indices showed that reservoir and conduit functions were slightly reduced with TKIs. Booster pump function did not change significantly. No significant correlations were noted between dynamic global LA/RA function indices and variables of LV/RV systolic and diastolic functions (data not shown).

Global Atrial Function Utilizing Deformation Indices

LA deformation indices of dynamic global function were similar with TKIs. On the other hand, RA conduit function was slightly reduced while reservoir function showed a trend but no significant decline with TKIs. Booster pump function did not change with TKIs (Table 5). No significant correlations were observed between LA/RA deformation indices and parameters of LV/RV systolic and diastolic functions (data not shown).

The assessment of intra- and interobserver variability documented fair correlation for indices of global and regional cardiac chambers function (Figure 3).

DISCUSSION

To the best of our knowledge, this is the first study in the literature addressing all cardiac chamber deformation in a single cohort as well as the potential subclinical hazardous effects of TKIs on cardiac function in patients with mRCC. The principal findings of this study are: (1) RV peak systolic GLε and SR significantly decreased post-TKIs; (2) LV peak systolic GLε and SR were not statistically altered post-TKIs; (3) global S′ wave of the mitral valve was significantly lower after TKIs; (4) reservoir and conduit functions of the RA were slightly reduced with TKIs according to volumetric and deformation indices; (5) no

significant effects were noted with TKIs on dynamic LA function; and (6) LVEF as well as conventional indices of RV function did not change significantly with TKIs.

Mechanisms of Cardiotoxicity

The plausible mechanisms of cardiotoxicity caused by TKIs are not entirely explored, but mouse studies suggest that angiogenesis, in part mediated by VEGFR2 and platelet-derived growth factor receptor (PDFGRβ), maintains cardiac homeostasis. TKI inhibition leads to impairment of vascular endothelial signaling, mitochondrial dysfunction, and loss of myocyte contractility.[2–9] Patients are more susceptible to off-target side effects with wider inhibition of tyrosine kinases. Sunitinib, with a wide spectrum of tyrosine kinases inhibition, carries considerable cardiovascular risks compared with pazopanib with a narrow spectrum of inhibition, and bevacizumab, which principally antagonizes the VEGFR.[2–9]

Among our patients, 18% developed new onset hypertension and 9% had worsening of pre-existing hypertension while on therapy. Incidence of hypertension appears to be less striking than in other cohorts.[2–9] This might be explained by the small cohort number and wider employment of pazopanib, with its narrow spectrum of tyrosine kinases inhibition and lower cardiovascular risk than the very potent TKI sunitinib. Of note, no patient developed other forms of cardiotoxicity (i.e., CHF or drop of LVEF). This is presumably due to better control of hypertension and meticulous follow-up.

Ventricular Deformation Indices

We observed that LV peak systolic GLε/SR was not statistically altered after TKIs with preserved LVEF in the absence of any reported symptoms (Table 3). Thavendiranathan et al, [27] in their systematic review of 1,504 patients, indicated that peak systolic GLε, measured with speckle tracking echocardiography, seems to be the best parameter consistently detecting incipient myocardial injury during chemotherapy. They expressed that a 10% to 15% early reduction in GLε is the best index for the prediction of cardiotoxicity, defined as a CHF or LVEF reduction. Plana et al[28] distinguished relative percentage drop of GLε > 15% from baseline to be abnormal. Our cohort showed no significant change in GLε/SR after TKIs therapy.

Global S′ wave of the mitral valve was significantly reduced after TKIs (Table 2). Impaired tissue Doppler indices, essentially S′ wave of the mitral valve, have been observed in early and late phases of follow-up in patients with breast cancer treated with anthracycline and trastuzumab.[28–30] However, the implication as a potential predictor of systolic function post-chemotherapy still needs to be explored.[28]

There was no significant change in conventional indices of RV systolic and diastolic function, principally FAC%, TAPSE, global S′ wave of the tricuspid valve, and RV systolic pressure as recommended by the expert report from the American Society of Echocardiography[28] (Table 2). However, RV peak systolic GLε and SR were significantly reduced post-TKIs in the absence of any signs of pulmonary hypertension (Table 3). Kocabaş, et al,[31] using tissue Doppler indices, noted that the RV was more susceptible to diastolic dysfunction, whereas the LV was more prone to systolic dysfunction in 72 children with cancer under low anthracycline dose. Oliveira et al[32] analyzed 3,812 mechanical

circulatory support patients from the INTERMACS (Interagency Registry for Mechanically Assisted Circulatory Support) database. They compared patients with chemotherapy-induced cardiomyopathy to patients with nonischemic and ischemic cardiomyopathy. They perceived that chemotherapy-induced cardiomyopathy patients have significant markers of RV dysfunction, lower pulmonary pressure, and higher need for RV assist device support in comparison to the remaining cardiomyopathy groups.[32] Our study uncovered noticeable reduction of RV indices in comparison to the LV indices. This ensured better sensitivity of deformation relative to conventional indices in detecting incipient RV dysfunction. Based on our cohort, together with the abovementioned studies, the RV is likely more vulnerable to chemotherapy than the LV in the absence of pulmonary hypertension and LV incipient dysfunction. We speculate that the RV has mainly longitudinal strain, which might be affected by TKIs. Conversely, LV has three strain components, including longitudinal, circumferential, and radial, which are participating in LV systolic function. In addition, RV has a thinner wall than the LV. This is the reason RV may have showed earlier involvement than LV. Also, the absence of LV circumferential and radial strain analysis and long-term follow-up might be a reason of unmasking LV incipient dysfunction hand in hand with RV dysfunction.[31–33]

Atrial Dynamic Function

Atrial function is an essential contributor of ventricular filling and has a prognostic implication in numerous cardiovascular diseases. The LA has three phasic components that reflect its dynamic function. Atrial reservoir function is defined as the capability of the LA to fill from the pulmonary veins during ventricular systole. Atrial conduit function matches the passive LV filling during early diastole and diastasis. Atrial booster pump or contractile function is related to the active atrial emptying at end diastole enhanced LV filling. The RA has three similar components. It has a dynamic share in RV filling. However, RA function has not been fully explored.[10,19–21,34–36]

According to volumetric and deformation indices, LA/RA volumes and EF as well as LA dynamic function indices were similar in both groups. On the other hand, RA reservoir and conduit functions were slightly reduced with TKIs with no significant change of booster pump function. Those finding are in keeping with and additive to the notion that the right side of the heart is more prone to damage secondary to chemotherapy than the left side (Tables 4 and 5).

Clinical Implications

This study provides further insights into the global influence of TKIs on the mechanical function of all cardiac chambers. Our data suggest that RV/LV deformation indices could be considered a diagnostic tool that may enable unmasking of incipient ventricular dysfunction in patients treated with TKIs. The study of atrial dynamic function is still in infancy, but it might have a prognostic significance. We recommend obtaining baseline and follow-up RV/LV indices for all patients on TKIs. The same algorithm might be applicable to atrial dynamic function if feasible. In case of development of subtle contractile dysfunction of any cardiac chamber, prompt decision regarding discontinuation of TKIs can be made before overt dysfunction or heart failure ensues. The impact of these conclusions and their potential

use will necessitate further study. Longer term study would be beneficial to assess whether LVEF or RVEF decline can be predicted by these findings.

Limitations

This study has limitations that deserve comment. It is a retrospective small cohort at a single institution. However, we noted differences in several variables. VVI of the atria is more complex and time-demanding than for the ventricles. VVI software is optimized for analysis of the ventricles and the use of the software for atrial deformation requires further validation. Our values are not similar to those of other investigators. This is presumably due to the use of VVI for analysis, whereas the majority of other studies applied the EchoPac software for image analysis by speckle tracking (Vingmed; GE-Healthcare, Horten, Norway).[19] No subgroup analysis was obtained to delineate the impact of individual TKI, new onset hypertension, RCC subtype, or TNM classification on deformation indices due to the small cohort. Additional imaging of cardiac chambers' myocardium, applying cardiac magnetic resonance, might be indicated to detect structural changes and lend support to our data. Finally, our median follow-up was 169 days to ensure completeness of TTE data, and no long-term follow-up was conducted to detect late effects of TKIs on deformation.

CONCLUSIONS

The influence of TKIs on all cardiac chambers in mRCC patients, treated in the short to intermediate term, shows that the right side of the heart exhibited greater changes in strain after TKI treatment than the left-sided chambers. The implication of these findings and their potential significance warrants further study, which is also necessary to assess the longer term effects.

Acknowledgments

Disclosures: T.H.H. is supported by funding from the Gloria A. and Thomas J. Dutson Jr. Kidney Research Endowment, a Kathryn H. and Roger Penske Career Development Award to Support Medical Research, and a US National Institutes of Health Grant K12CA90628. The funders had no role in study design, data collection and analysis, decision to publish, or preparation of the manuscript.

REFERENCES

1. Escudier B, Porta C, Schmidinger M, et al. ESMO Guidelines Working Group. Renal cell carcinoma: ESMO Clinical Practice Guidelines for diagnosis, treatment and follow-up. Ann Oncol 2014;25(Suppl 3):iii49. [PubMed: 25210086]
2. Di Lorenzo G, Autorino R, Bruni G, et al. Cardiovascular toxicity following sunitinib therapy in metastatic renal cell carcinoma: a multicenter analysis. Ann Oncol 2009;20:1535. [PubMed: 19474115]
3. Hall PS, Harshman LC, Srinivas S, et al. The frequency and severity of cardiovascular toxicity from targeted therapy in advanced renal cell carcinoma patients. JACC Heart Fail 2013;1:72. [PubMed: 24621801]
4. Zuppinger C, Suter TM. Cancer therapyassociated cardiotoxicity and signaling in the myocardium. J Cardiovasc Pharmacol 2010;56:141. [PubMed: 20386457]
5. Verkhivker GM. Exploring sequence-structure relationships in the tyrosine kinome space: functional classification of the binding specificity mechanisms for cancer therapeutics. Bioinformatics 2007;23:1919. [PubMed: 17537753]

6. Izumiya Y, Shiojima I, Sato K, et al. Vascular endothelial growth factor blockade promotes the transition from compensatory cardiac hypertrophy to failure in response to pressure overload. Hypertension 2006;47:887. [PubMed: 16567591]
7. Pantaleo MA, Mandrioli A, Saponara M, et al. Development of coronary artery stenosis in a patient with metastatic renal cell carcinoma treated with sorafenib. BMC Cancer 2012;12:231. [PubMed: 22687270]
8. Schutz FA, Je Y, Richards CJ, et al. Meta-analysis of randomized controlled trials for the incidence and risk of treatment-related mortality in patients with cancer treated with vascular endothelial growth factor tyrosine kinase inhibitors. J Clin Oncol 2012;30:871. [PubMed: 22312105]
9. Chintalgattu V, Ai D, Langley RR, et al. Cardiomyocyte PDGFR-beta signaling is an essential component of the mouse cardiac response to load-induced stress. J Clin Invest 2010;120:472. [PubMed: 20071776]
10. Moustafa SE, Alharthi M, Kansal M, et al. Global left atrial dysfunction and regional heterogeneity in primary chronic mitral insufficiency. Eur J Echocardiogr 2011;12:384. [PubMed: 21447498]
11. Moustafa SE, Kansal M, Alharthi M, et al. Prediction of incipient left ventricular dysfunction in patients with chronic primary mitral regurgitation: a velocity vector imaging study. Eur J Echocardiogr 2011;12:291. [PubMed: 21343164]
12. Deng Y, Alharthi MS, Thota VR, et al. Evaluation of left ventricular rotation in obese subjects by velocity vector imaging. Eur J Echocardiogr 2010; 11:424. [PubMed: 20190270]
13. Pirat B, Khoury DS, Hartley CJ, et al. A novel feature-tracking echocardiographic method for the quantitation of regional myocardial function: validation in an animal model of ischemia-reperfusion. J Am Coll Cardiol 2008;51:651. [PubMed: 18261685]
14. Jarnert C, Melcher A, Caidahl K, et al. Left atrial velocity vector imaging for the detection and quantification of left ventricular diastolic function in type 2 diabetes. Eur J Heart Fail 2008;10:1080. [PubMed: 18838296]
15. Burri MV, Nanda NC, Lloyd SG, et al. Assessment of systolic and diastolic left ventricular and left atrial function using vector velocity imaging in Takotsubo cardiomyopathy. Echocardiography 2008;25:1138. [PubMed: 18986398]
16. Lang RM, Badano LP, Mor-Avi V, et al. Recommendations for cardiac chamber quantification by echocardiography in adults: an update from the American Society of Echocardiography and the European Association of Cardiovascular Imaging. J Am Soc Echocardiogr 2015;28:1. [PubMed: 25559473]
17. Lang RM, Bierig M, Devereux RB, et al. Recommendations for chamber quantification: a report from the American Society of Echocardiography's Guidelines and Standards Committee and the Chamber Quantification Writing Group. Eur J Echocardiogr 2006;7:79. [PubMed: 16458610]
18. Rudski LG, Lai WW, Afilalo J, et al. Guidelines for the echocardiographic assessment of the right heart in adults: a report from the American Society of Echocardiography endorsed by the European Association of Echocardiography, a registered branch of the European Society of Cardiology, and the Canadian Society of Echocardiography. J Am Soc Echocardiogr 2010;23:685. [PubMed: 20620859]
19. Mor-Avi V, Lang RM, Badano LP, et al. Current and evolving echocardiographic techniques for the quantitative evaluation of cardiac mechanics: ASE/EAE consensus statement on methodology and indications endorsed by the Japanese Society of Echocardiography. Eur J Echocardiogr 2011;12: 167. [PubMed: 21385887]
20. Peluso D, Badano LP, Muraru D, et al. Right atrial size and function assessed with three-dimensional and speckle-tracking echocardiography in 200 healthy volunteers. Eur Heart J Cardiovasc Imaging 2013;14:1106. [PubMed: 23423966]
21. Kutty S, Padiyath A, Li L, et al. Functional maturation of left and right atrial systolic and diastolic performance in infants, children, and adolescents. J Am Soc Echocardiogr 2013;26:398. [PubMed: 23337737]
22. Caso P, Ancona R, Di Salvo G, et al. Atrial reservoir function by strain rate imaging in asymptomatic mitral stenosis: prognostic value at 3 year follow-up. Eur J Echocardiogr 2009;10:753. [PubMed: 19443469]

23. Okamatsu K, Takeuchi M, Nakai H, et al. Effects of aging on left atrial function assessed by two-dimensional speckle tracking echocardiography. J Am Soc Echocardiogr 2009;22:70. [PubMed: 19131005]
24. Vianna-Pinton R, Moreno CA, Baxter CM, et al. Two-dimensional speckle-tracking echocardiography of the left atrium: feasibility and regional contraction and relaxation differences in normal subjects. J Am Soc Echocardiogr 2009;22:299. [PubMed: 19258177]
25. Sirbu C, Herbots L, D'hooge J, et al. Feasibility of strain and strain rate imaging for the assessment of regional left atrial deformation: a study in normal subjects. Eur J Echocardiogr 2006;7:199. [PubMed: 16054869]
26. Spencer KT, Mor-Avi V, Gorcsan J 3rd, et al. Effects of aging on left atrial reservoir, conduit, and booster pump function: a multi-institution acoustic quantification study. Heart 2001;85:272. [PubMed: 11179264]
27. Thavendiranathan P, Poulin F, Lim KD, et al. Use of myocardial strain imaging by echocardiography for the early detection of cardiotoxicity in patients during and after cancer chemotherapy: a systematic review. J Am Coll Cardiol 2014;63:2751. [PubMed: 24703918]
28. Plana JC, Galderisi M, Barac A, et al. Expert consensus for multimodality imaging evaluation of adult patients during and after cancer therapy: a report from the American Society of Echocardiography and the European Association of Cardiovascular Imaging. J Am Soc Echocardiogr 2014;27: 911. [PubMed: 25172399]
29. Fallah-Rad N, Walker JR, et al. The utility of cardiac biomarkers, tissue velocity and strain imaging, and cardiac magnetic resonance imaging in predicting early left ventricular dysfunction in patients with human epidermal growth factor receptor II-positive breast cancer treated with adjuvant trastuzumab therapy. J Am Coll Cardiol 2011;57:2263. [PubMed: 21616287]
30. Ho E, Brown A, Barrett P, et al. Subclinical anthracycline- and trastuzumab-induced cardiotoxicity in the long-term follow-up of asymptomatic breast cancer survivors: a speckle tracking echocardiographic study. Heart 2010;96:701. [PubMed: 20424152]
31. Kocabaş A, Kardelen F, Ertug H, et al. Assessment of early-onset chronic progressive anthracycline cardiotoxicity in children: different response patterns of right and left ventricles. Pediatr Cardiol 2014;35:82. [PubMed: 23821296]
32. Oliveira GH, Dupont M, Naftel D, et al. Increased need for right ventricular support in patients with chemotherapy-induced cardiomyopathy undergoing mechanical circulatory support: outcomes from the INTERMACS Registry (Interagency Registry for Mechanically Assisted Circulatory Support). J Am Coll Cardiol 2014;63:240. [PubMed: 24161324]
33. Moustafa S, Murphy K, Nelluri BK, et al. Temporal trends of cardiac chambers function with trastuzumab in human epidermal growth factor receptor II-positive breast cancer patients. Echocardiography 2015 (Epub ahead of print).
34. Moustafa S, Zuhairy H, Youssef MA, et al. Right and left atrial dissimilarities in normal subjects explored by speckle tracking echocardiography. Echocardiography 2015;32:1392. [PubMed: 25611312]
35. Rosca M, Lancellotti P, Popescu BA, et al. Left atrial function: pathophysiology, echocardiographic assessment, and clinical applications. Heart 2011;97:1982. [PubMed: 22058287]
36. Gaynor SL, Maniar HS, Prasad SM, et al. Reservoir and conduit function of right atrium: impact on right ventricular filling and cardiac output. Am J Physiol Heart Circ Physiol 2005;288:H2140.

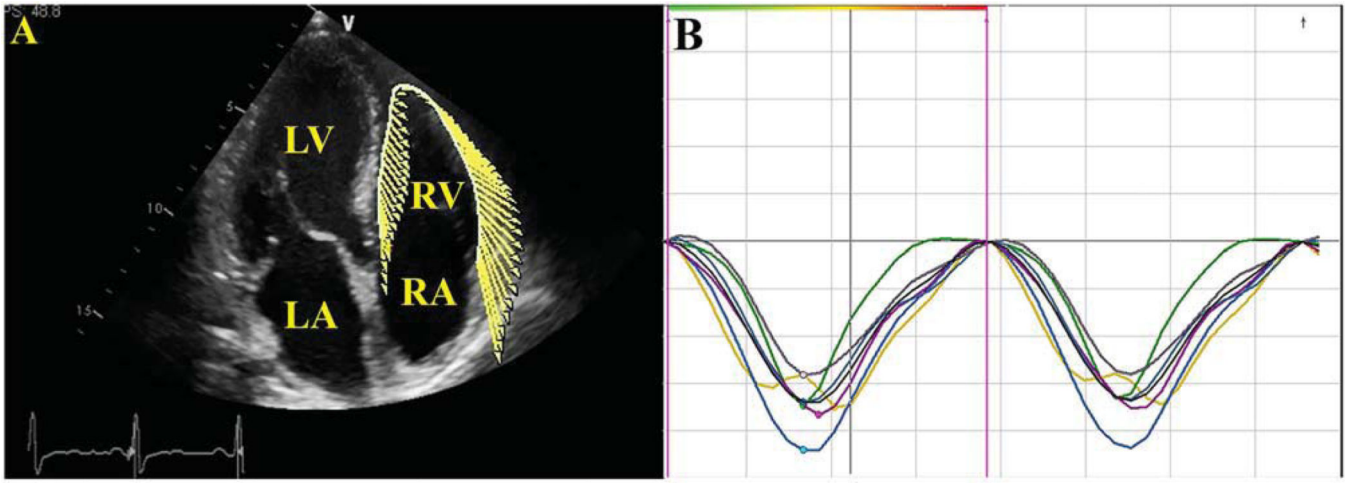

FIGURE 1.

(**A**) Tracing of the right ventricle (RV) endocardial border in apical four-chamber view. (**B**) Strain versus time curves. LA, left atrium; LV, left ventricle; RA, right atrium.

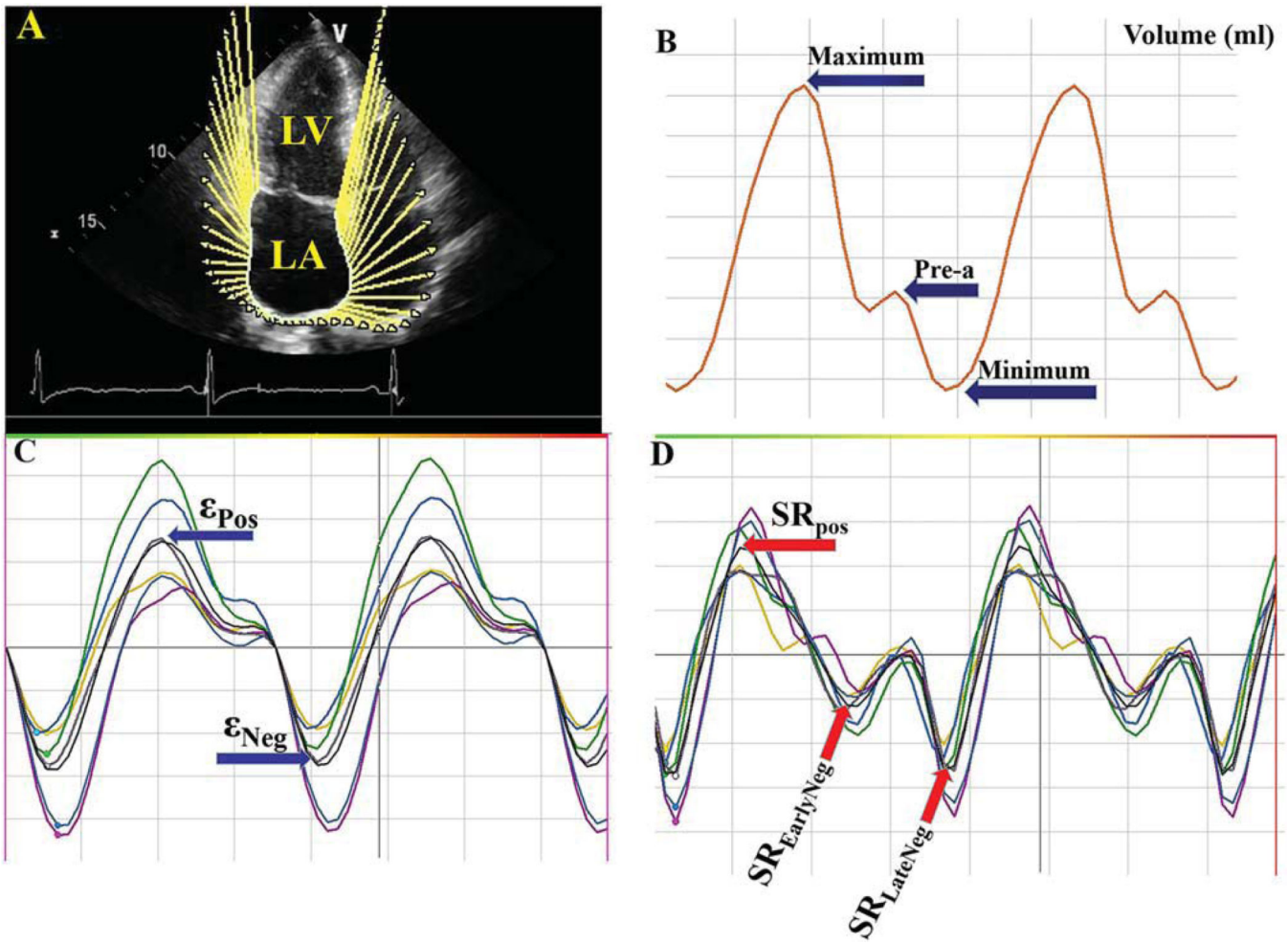

FIGURE 2.

Example of assessment of left atrium (LA) volumes and strain (ε)/strain rate (SR). (**A**) Tracing of the LA endocardial border in the apical four-chamber view. (**B**) Maximum, minimum, and preatrial contraction volumes were computed from the generated volume curve. (**C, D**) ε and SR versus time curves. LV, left ventricle; Pre-A, pre-atrial contraction volume; ε_{Pos}, peak positive ε; ε_{Neg}, peak negative ε; $SR_{EarlyNeg}$, peak early negative SR; $SR_{LateNeg}$, peak late negative SR; SR_{Pos}, peak positive SR.

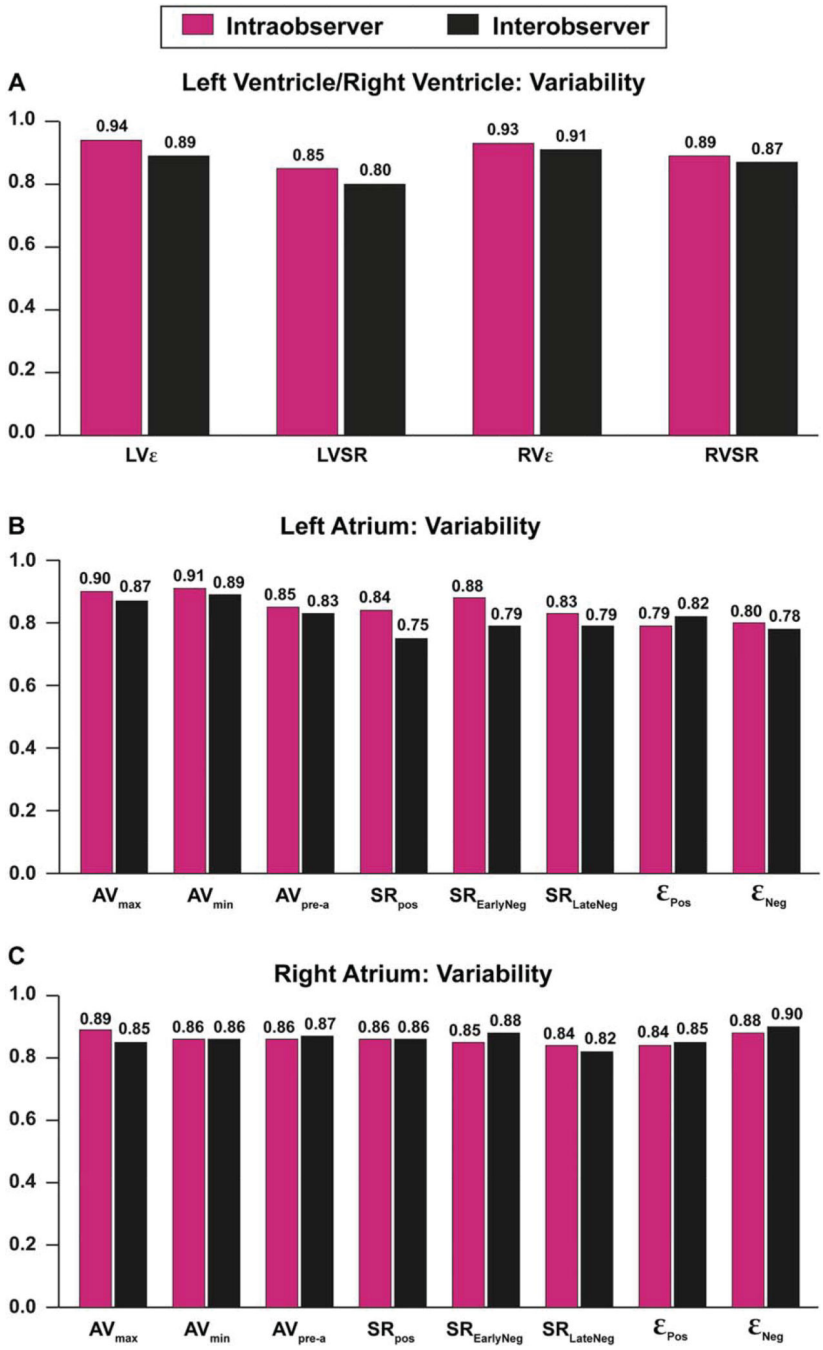

FIGURE 3.

Intra- and interobserver agreement of the left/right ventricles (**A**), left atrium (**B**), and right atrium (**C**) measurements. AVmax, maximum atrial volume; AVmin, minimal atrial volume; AVpre-a, atrial volume before the atrial contraction; ε_{Pos}, peak positive ε; ε_{Neg}, peak negative ε; LVε, left ventricle E; LVSR, left ventricular strain rate; RVε, right ventricle ε; RVSR, right ventricular strain rate; $SR_{EarlyNeg}$, peak early negative SR; $SR_{LateNeg}$, peak late negative SR; SR_{Pos}, peak positive SR.

TABLE 1

Baseline Clinical Characteristics of the Study Population

	Study Population (N = 23)
Age, years	67 ± 9
Men (%)	21 (92)
Height (cm)	174 ± 7.9
Weight (kg)	86.7 ± 14.7
Body surface area (m^2)	2.01 ± 0.18
Body mass index (kg/m^2)	28.4 ± 4.3
Heart rate (bpm)	68 ±12
Systolic blood pressure (mmHg)	132 ± 14
Diastolic blood pressure (mmHg)	77 ±9
Risk factors	
Hypertension (%)	10 (43)
Diabetes mellitus (%)	2 (9)
Dyslipidemia (%)	14 (61)
Coronary artery disease (%)	3 (13)
TKIs	
Pazopanib (%)	15 (65)
Sunitinib (%)	6 (26)
Axitinib (%)	2 (9)
Cardiac medications	
Beta-blockers (%)	9 (39)
Calcium channel blockers (%)	4 (18)
Angiotensin converting enzyme inhibitors (%)	4 (18)
Angiotensin receptors blockers (%)	1 (4.5)
Statins (%)	10 (43)
Aspirin (%)	7 (30)

Abbreviation: TKIs, tyrosine kinase inhibitors.

TABLE 2

Echocardiographic Characteristics of the Study Population

	Pre-TKIs	Post-TKIs	*p* Value
LAVI (ml/m^2)	27.9 ± 7.6	27.6 ± 8.6	0.44
LV end-diastolic diameter (mm)	47.9 ± 4.2	46.5 ± 5.9	0.18
LV end-systolic diameter (mm)	30.1 ± 3.9	30.2 ± 6.5	0.48
Septal wall thickness (mm)	11.2 ± 2.1	11.3 ± 2.1	0.41
Posterior wall thickness (mm)	10.5 ± 1.8	10.5 ± 1.9	0.35
LV mass index (g/m^2)	93.7 ± 24.2	93.9 ± 21.2	0.42
LVEF (%)	61.5 ± 6.1	59.7 ± 7.1	0.14
E wave (m/s)	0.66 ± 0.15	0.63 ± 0.25	0.28
A wave (m/s)	0.69 ± 0.21	0.68 ± 0.19	0.38
E/A ratio	0.95 ± 0.34	0.88 ± 0.35	0.28
E deceleration time (msec)	228.4 ± 42.3	213.4 ± 70.6	0.2
E′ wave (m/sec) *	0.07 ± 0.03	0.06 ± 0.02	0.07
A′ wave (m/sec) *	0.09 ± 0.025	0.08 ± 0.02	0.16
S′ wave (m/sec) *	0.08 ± 0.2	0.07 ± 0.02	0.02
E/E′ ratio *	10.1 ± 4.5	11.4 ± 7.4	0.18
LV MPI (pulsed Doppler)	0.29 ± 0.08	0.29 ± 0.09	0.47
RA end systolic area (cm^2)	15.2 ± 3.9	13.6 ± 3.5	0.06
RA major diameter (mm)	49.2 ± 5.5	49.2 ± 5.3	0.46
RA minor diameter (mm)	36.9 ± 5.1	34.6 ± 5.1	0.08
RV basal diameter (mm)	35.4 ± 5.9	33.1 ± 5.5	0.1
RVOTP	30.8 ± 4.4	30.5 ± 3.8	0.45
RVOTD	22.4 ± 4.1	23.1 ± 3.4	0.18
RV subcostal wall thickness (mm)	56 ± 12	52 ± 10	0.08
RV FAC (%)	48.8 ± 8.5	48.4 ± 7.3	0.32
TAPSE (mm)	22.9 ± 3.9	22.2 ± 4.6	0.41
Tricuspid E wave (m/s)	0.52 ± 0.09	0.54 ± 0.11	0.4
Tricuspid A wave (m/s)	0.49 ± 0.14	0.49 ± 0.1	0.4
Tricuspid E/A ratio	1.12 ± 0.26	1.14 ± 0.31	0.28
Tricuspid E deceleration time (msec)	188. ± 58.2	197.3 ± 57.2	0.2
Tricuspid E′ wave (m/sec)	0.09 ± 0.04	0.09 ± 0.03	0.4
Tricuspid A′ wave (m/sec)	0.12 ± 0.04	0.11 ± 0.04	0.3
Tricuspid S wave (m/sec)	0.12 ± 0.03	0.11 ± 0.02	0.2
Tricuspid E/E′ ratio	0.77 ± 0.34	0.79 ± 0.29	0.2
RV MPI (pulsed Doppler)	0.28 ± 0.09	0.29 ± 0.08	0.17
RVSP (mmHg)	28.9 ± 7.9	30.8 ± 7.9	0.5

Values are expressed as mean ± SD.

Abbreviations: E, peak early filling transmitral velocity; A, peak late filling transmitral velocity; E′, peak longitudinal early diastolic tissue velocity of the mitral valve annulus; A′, peak longitudinal late diastolic tissue velocity of the mitral valve annulus; LA, left atrium; LAVI, indexed LA

volume; LV, left ventricle; LVEF, left ventricular ejection fraction; RA, right atrium; RV, right ventricle; RV FAC, RV fractional area change; RVOTD, RV outflow tract distal; RVOTP, RV outflow tract proximal; TAPSE, tricuspid annular plane systolic excursion; RVSP, RV systolic pressure; MPI, myocardial performance index.

* Values represent the average of medial and lateral velocities.

TABLE 3

Aspects of Left Ventricle (LV)/Right Ventricle (RV) Function Assessed by Deformation Indices

	Pre-TKIs	Post-TKIs	*p* Value
Left ventricle			
GLε (%)	−16.53 ± 2.81	−15.69 ± 2.92	0.076
% change of GLε		−5.3%	
SR (s^{-1})	−1.01 ± 0.35	−0.95 ± 0.25	0.19
Right ventricle			
GLε (%)	−23.49 ± 5.1	−19.81 ± 5.5	0.002
% change of GLε		−15.6%	
SR (s^{-1})	−1.52 ± 0.52	−1.24 ± 0.35	0.02

Abbreviations: GLε, Global longitudinal strain; SR, strain rate.

TABLE 4

Aspects of Atrial Function Assessed by Volumetric Indices

	Pre-TKIs	Post-TKIs	*p* Value
Left atrium			
AVmax (ml)	60.2 ± 22.3	53.8 ± 27.6	0.12
AVmax/BSA (ml/m^2)	29.8 ± 10.4	26.8 ± 13.1	0.12
AVmin (ml)	22.6 ± 13.4	20.1 ± 12.6	0.18
AVmin/BSA (ml/m^2)	11.11 ± 6.2	9.9 ± 5.9	0.18
AVpre-a (ml)	41.1 ± 20.9	36.8 ± 20.3	0.14
AVpre-a/BSA (ml/m^2)	20.3 ± 9.9	18.3 ± 9.6	0.14
Atrial ejection fraction (%)	64 ± 12.4	61.8 ± 13.3	0.21
Atrial reservoir function			
1. Filling volume (ml)	37.6 ± 13.1	33.6 ± 18.1	0.14
2. Expansion index (%)	59.2 ± 22.2	52.8 ± 27.6	0.12
3. Diastolic emptying index	59.8 ± 22.2	53.4 ± 27.5	0.12
Atrial conduit function			
1. Passive emptying (%) of total emptying	36.9 ± 13.1	32.9 ± 18.1	0.14
2. Passive emptying index	59.5 ± 22.2	53.1 ± 27.6	0.12
Atrial booster pump function			
1. Active emptying (%) of total emptying	18.1 ± 9.2	16.3 ± 11.1	0.15
2. Active emptying index	40.5 ± 20.9	36.2 ± 20.3	0.14
Right atrium			
AVmax (ml)	52.5 ± 17.5	44.6 ± 17.1	0.052
AVmax/BSA (ml/m^2)	25.9 ± 8.3	22.4 ± 8.6	0.06
AVmin (ml)	21.7 ± 11.1	19.5 ± 9.6	0.15
AVmin/BSA (ml/m^2)	10.7 ± 4.9	9.8 ± 4.5	0.15
AVpre-a (ml)	36.2 ± 16.3	31.6 ± 14.1	0.12
AVpre-a/BSA (ml/m^2)	17.8 ± 7.5	15.9 ± 6.9	0.14
Atrial ejection fraction (%)	59.1 ± 12.8	56.3 ± 12.4	0.2
Atrial reservoir function			
1. Filling volume (ml)	30.8 ± 12.5	25.03 ± 11.3	0.041
2. Expansion index (%)	51.5 ± 17.5	43.6 ± 17.1	0.046
3. Diastolic emptying index	52.1 ± 17.5	44.1 ± 17.1	0.046
Atrial conduit function			
1. Passive emptying (%) of total emptying	30.1 ± 12.6	24.3 ± 11.4	0.04
2. Passive emptying index	51.8 ± 17.5	43.8 ± 17.1	0.46
Atrial booster pump function			
1. Active emptying (%) of total emptying	14.1 ± 9.7	11.6 ± 7.1	0.19
2. Active emptying index	35.5 ± 16.3	30.9 ± 14.1	0.12

Abbreviations: AVmax, maximum atrial volume; AVmin, minimal atrial volume; AVpre-a, atrial volume before the atrial contraction; BSA, body surface area.

TABLE 5

Aspects of Atrial Function Assessed by Deformation Indices

	Pre-TKIs	Post-TKIs	*p* Value
Left atrium			
Total longitudinal atrial ε (%)*	36.5 ± 16.6	31.53 ± 13.77	0.13
Atrial reservoir function			
SR_{pos}	1.26 ± 0.43	1.093 ± 0.47	0.09
Atrial conduit function			
$SR_{EarlyNeg}$	−0.93 ± 0.45	−0.77 ± 0.37	0.09
ε_{Pos}	34.3 ± 17.4	29.59 ± 13.42	0.14
Atrial booster pump function			
ε_{Neg}	−2.22 ± 2.53	−1.94 ± 3.59	0.32
$SR_{LateNeg}$	−1.04 ± 0.45	−0.92 ± 0.57	0.18
Right atrium			
Total longitudinal atrial ε (%)*	52.38 ± 22.1	43.12 ± 29.06	0.09
Atrial reservoir function			
SR_{pos}	1.47 ± 0.49	1.22 ± 0.49	0.058
Atrial conduit function			
$SR_{EarlyNeg}$	−1.19 ± 0.46	−0.95 ± 0.45	0.044
ε_{Pos}	51.05 ± 22.81	40.89 ± 29.79	0.07
Atrial booster pump function			
ε_{Neg}	−1.33 ± 2.07	−2.22 ± 2.81	0.12
$SR_{LateNeg}$	−1.26 ± 0.56	−1.03 ± 0.51	0.07

Abbreviations: TKIs, tyrosine kinase inhibitors; ε, strain; SR, strain rate; ε_{Pos}, peak positive ε; ε_{Neg}, peak negative ε; $SR_{EarlyNeg}$, peak early negative SR; $SR_{LateNeg}$, peak late negative SR; SR_{Pos}, peak positive SR.

*Calculated as the average value throughout the whole cardiac cycle.